

Influence of Filler Content on Static Properties of Glass-Reinforced Bone Cement

Claudia I. Vallo

Institute of Materials Science and Technology (INTEMA), Universidad Nacional de Mar del Plata—National Research Council (CONICET), Av. Juan B. Justo 4302, (7600) Mar del Plata, Argentina

Received 23 March 2000; revised 7 July 2000; accepted 19 July 2000

Abstract: A commercial acrylic bone cement was modified by the incorporation of different weight fractions of glass spheres. The influence of the filler proportion on the mechanical behavior was assessed. Composite cements were prepared by replacing part of the powder phase of the cement by an equivalent weight of glass particles, which resulted in an increase in the liquid-to-powder (L/P) ratio of the polymeric matrix. Dynamic mechanical analysis revealed an increase in residual monomer content with increasing filler proportion as a consequence of the increase in L/P. Flexural, compressive, and fracture properties of the cement with varying amounts of glass particles were measured. It was found that up to 50 wt% glass particles could be added with significant increases in flexural modulus and fracture toughness. The mechanical behavior was explained in terms of both the reinforcing effect of the filler and the plasticizing effect of the monomer. Glass-filled bone cements displayed superior workability compared with the standard cement, which was attributed to a decrease in the viscosity of the initial mix and the surface characteristics of the glass particles. The observed increase in fracture toughness could be rationalized through the application of proposed mechanisms for toughening of particle-reinforced polymers. © 2000 John Wiley & Sons, Inc. *J Biomed Mater Res (Appl Biomater)* 53: 717–727, 2000

Keywords: acrylic bone cements; particle-reinforced composite bone cements; particulate glass filler; residual monomer; mechanical properties

INTRODUCTION

Poly(methyl methacrylate) (PMMA) based bone cement is widely used in orthopedics to fix joint replacements into the bone. Numerous studies have suggested deficiencies in the mechanical properties of currently used bone cement.¹ Given the large number of total hip replacement operations performed annually, then even a relatively small failure rate has important implications in terms of the need for revision operations.

Various approaches to enhance the mechanical properties of bone cements are reported in the literature. Modification of the mixing methods of existing commercial PMMA bone cements was the focus of much research.^{2–5} Centrifugation and vacuum mixing were suggested as methods to improve the mechanical properties.^{5–9} These improvements were attributed to the markedly reduced porosity and reduction in pore size in the hardened material. Porosity, pore size, and

pore-size distribution were considered the main reasons for the lower strength of surgical-grade PMMA compared with industrial grade PMMA. Beaumont et al.¹⁰ reported that plane strain fracture toughness, K_{IC} , increased with the fabrication pressure of the samples, which controls the void content of the cement.

On the other hand, some studies concentrated on the incorporation of a second reinforcing phase to the cement. Although significant improvement on the mechanical properties is possible through the incorporation of fiber-reinforcing phases,^{11–14} previous studies have shown that the flow characteristics of the resultant composite are severely compromised. This has led to studies of particulate-filled composite bone cements^{15–24} that offer the possibility of improved mechanical properties without severe reductions in flow characteristics of the precured polymers. The present investigation explored this approach through the incorporation of glass particles within a bone cement. Silicate glasses of a wide range of compositions have been shown to be biocompatible and are used in dental applications.²⁵ Thus, glass spheres were used as the fillers in the present work.

Bone cements are prepared by mixing powdered prepolymerized PMMA beads with liquid methyl methacrylate (MMA) monomer in a proportion of liquid to powder (L/P) equal to 0.5. When adding particulate fillers to a bone cement,

Correspondence to: Claudia I. Vallo, Institute of Materials Science and Technology (INTEMA), Universidad Nacional de Mar del Plata—National Research Council (CONICET), Av. Juan B. Justo 4302, (7600) Mar del Plata, Argentina (e-mail: civallo@fi.mdp.edu.ar)

Contract grant sponsor: National Research Council (CONICET)

© 2000 John Wiley & Sons, Inc.

the maximum amount that can be incorporated is limited by the viscosity of the initial mix. Highly viscous initial mix results in both poor workability of the paste and high porosity of the hardened material. From the analysis of the results reported by previous workers, it emerges that some authors incorporated the filler maintaining the L/P ratio equal to 0.5,¹⁵⁻¹⁸ while others prepared composite cements by replacing part of the PMMA powder by the filler.¹⁹⁻²² The latter method allows the addition of a higher amount of filler without jeopardizing the workability of the cement. Along this same line, composite cements were prepared by replacing part of the PMMA powder by an equivalent weight of glass particles.

The objective of the present work was to study the effect of different amounts of glass particles on the mechanical properties of the resulting glass-filled bone cement. The mechanical characterization of the composite cements was accomplished by the measurement of flexural modulus of elasticity, compressive yield strength, and fracture toughness. The method of composite cements preparation resulted in an increase in the L/P ratio of the polymeric matrix with an increasing amount of filler. Therefore, changes in the mechanical behavior of the polymeric matrix produced by the addition of filler were evaluated.

Beaumont²⁶ and Owen et al.²⁷ studied the influence dispersions of various amounts of Barium Sulphate (BaSO_4) on the crack propagation and fracture processes on surgical acrylic bone cements. The authors found that the presence of BaSO_4 had a marked effect on the mode of fracture. In the present work, a radiolucent cement (without BaSO_4) was used to eliminate the influence of BaSO_4 particles that might overlap the effect of the glass filler.

Differential scanning calorimetry and dynamic mechanical analysis were conducted to determine the influence of the L/P ratio on the residual monomer content. The mechanical behavior observed was explained in terms of the reinforcing effect of the filler and the changes produced in the polymeric matrix as a consequence of the variation in L/P. The fracture mechanisms were also analyzed. Fractured surfaces were examined using scanning electron microscopy and documented in representative photomicrographs.

MATERIALS AND METHODS

Materials

A commercially available standard viscosity bone cement, Subiton (Subiton Laboratories, Buenos Aires, Argentina) was employed. As reported by the supplier, each dose of surgical bone cement consisted of 40 g of PMMA powder and 20 g of liquid monomer. The liquid component is composed of 19.76 g MMA monomer, 0.24 g *N,N*-dimethyl-*p*-toluidine and 18–20 ppm hydroquinone. The solid component is composed of 39.03 g PMMA and 0.97 g benzoyl peroxide. BaSO_4 is usually added to the PMMA powder to impart radiopacity to the cement. However, in the present work, a radiolucent

TABLE I. Mixing Composition of Glass Reinforced Bone Cement

| Glass Filler (wt%) | PMMA Powder (grams) | Glass Filler (grams) | MMA (grams) | L/P |
|--------------------|---------------------|----------------------|-------------|------|
| 12.5 | 35 | 5 | 20 | 0.57 |
| 25 | 30 | 10 | 20 | 0.67 |
| 37.5 | 25 | 15 | 20 | 0.80 |
| 50 | 20 | 20 | 20 | 1.00 |

cement (without BaSO_4) was used to eliminate the influence of BaSO_4 particles that might overlap the effect of the filler. Glass spheres having diameters in the 105–210 μm range were used as filler. They were given no special surface pretreatment, but were cleaned with isopropanol and dried at 100°C before molding to remove any contaminants. Different weight fractions of glass spheres were achieved by removing PMMA polymer from the powder and replacing it with an equal weight of glass particles. A 2:1 powder-to-liquid ratio as specified by the cement manufacturer was used when forming the composite cements, but the mass of powder included the PMMA and filler particles. The amount of each component is summarized in Table I. L/P is the MMA/PMMA ratio.

Mechanical Properties

Flexural, compressive, and fracture tests were carried out at room temperature in a Shimadzu Autograph S-500-C Universal testing machine at a cross-head displacement rate of 2 mm/min. The mechanical properties measured were the flexural modulus of elasticity (E), the compressive yield strength (σ_y), and the fracture toughness (K_{IC}).

All samples were prepared in the same way to avoid the eventual influence of the preparation technique upon mechanical properties. Blending of the PMMA powder and glass particles was accomplished in a ball mill for 2 h. Both components (liquid and powder), were chilled to 5°C before mixing, and then they were mixed slowly by hand for 0.5 min. Following mixing, the cement was immediately poured into molds to prepare specimens for subsequent mechanical characterization. All samples were allowed to cure at room temperature and an additional set was also postcured at 130°C for 2 h. The postcuring treatment at high temperature increases the diffusion and mobility of the residual monomer, thus making it easier for the monomer to either leach out of the cement or for continued curing to occur.

Plates for flexure and fracture specimens were obtained by casting the mixture into molds consisting of two rectangular glass plaques spaced by a rubber cord and held together with clamps. Test specimens were produced by cutting slabs into beams using a diamond saw.

The Young's modulus was measured in flexure. Results were computed using the standard formula:

$$E = L^3P/4bd^3y,$$

where E is the Young's modulus, L is the length between the supports, P is the load, b is the width of the specimen, d is the thickness of the specimen, and y is the deflection at the center. Flexural moduli were determined using sample dimensions recommended by the ASTM D790. The results are the average of five measurements.

Samples for compression testing were made by injecting the mix into polypropylene cylindrical disposable molds of 6 mm internal diameter. After removal from the molds, the compression specimens were machined to reach their final dimensions. Cylindrical specimens having an aspect ratio of 2 were deformed between metallic plates lubricated with molybdenum disulfide. True stress-deformation curves were obtained by dividing the load by the original cross-sectional area and converting it into true stress, assuming constant volume deformation. The deformation was calculated directly from the cross-head speed. The yield stress was determined at the maximum load. The results are the average of five measurements.

Fracture mechanics measurements were made in 3-point bending. The fracture toughness of each cement was characterized through the critical stress intensity factor, K_{IC} , calculated from:

$$K_{IC} = \sigma_c (\pi a)^{1/2} f(a/W)$$

where $\sigma_c = 3P_c L / (2b^2W)$ is the critical stress for crack propagation, P_c is the load at fracture, L is the span between supports, b is the thickness, W is the width, a is the initial crack length, and $f(a/W)$ is a calibration factor. For this geometry, $f(a/W)$ is given by²⁸:

$$f(a/W) = 1.09 - 1.735(a/W) + 8.2(a/W)^2 - 14.18(a/W)^3 + 14.57(a/W)^4$$

Central V notches were machined in the bars and extended by tapping a fresh razor blade into the tip of the notch to give a crack length range of $0.45 < a/W < 0.55$. The span to width (L/W) ratio was always equal to 4. The length of the initial crack, a , was measured from the fracture surface using a profile projector with a magnification of 10, averaging the results in five points as suggested by ASTM E399 standard. A minimum of eight specimens were tested.

Differential Scanning Calorimetry

The calorimetric measurements were made with a Shimadzu TA 50 calorimeter. Samples (8–10 mg) taken from plaques cured at room temperature were sealed in hermetic aluminum pans and tested immediately. Runs were carried out from 20–150°C at a heating rate of 10°C/min under a nitrogen flow, and an empty capsule served as reference. The variation of rate of heat output as a function of time and temperature was obtained on a chart recorder. The sample pans were reweighed after completion of the test to determine any loss of monomer during the measurements.

Dynamic Mechanical Properties

The dynamic mechanical properties were studied using a Perkin–Elmer DMA 7-e in the 3-point bending mode. Each sample was scanned from 0–150°C at a heating rate of 10°C per min. During heating, the samples were subjected to strain at a frequency of 1 Hz, while the storage modulus (E'), the damping factor ($\tan \delta$) and probe position were recorded.

Scanning Electron Microscopy

Fracture surfaces were examined by scanning electron microscopy (SEM) using a Jeol JSM 35 CF apparatus, after coating the broken surfaces with a thin gold layer.

RESULTS AND DISCUSSION

The flexural modulus, the compressive yield strength, and the fracture toughness were measured in samples cured at room temperature and samples subjected to a postcuring treatment at 130°C in order to assess the influence of the unreacted monomer on the mechanical behavior of the composite cements.

The flexural test results are shown in Figure 1. It is observed that a significant increase in the flexural modulus (E) increases filler content. By the addition of 50 wt% filler, the flexural modulus of samples cured at room temperature increased by approximately 68% compared with the unreinforced cement. Beaumont¹⁵ studied the strength and toughness of acrylic bone cements containing a second phase dispersion of glass spheres. Measurements of Young modulus, E , as a function of glass content demonstrated that E increased monotonically while increasing the filler content, which is in agreement with the results observed in the present work. The samples cured at room temperature displayed lower flexural modulus than the samples subjected to a post-

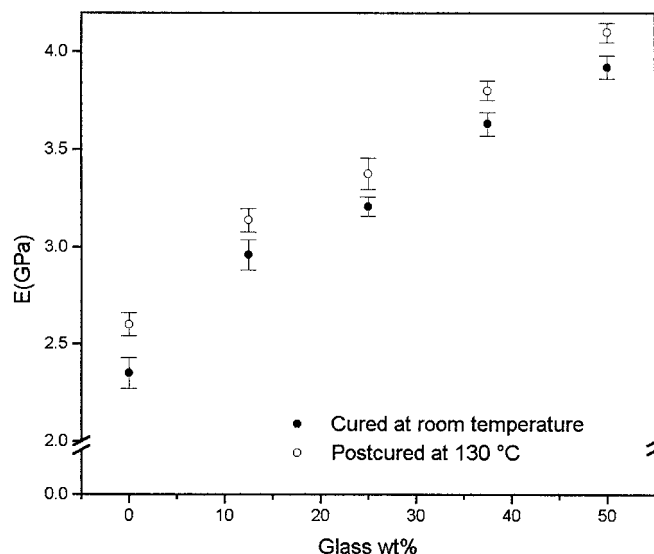


Figure 1. Flexural modulus vs. wt% glass.

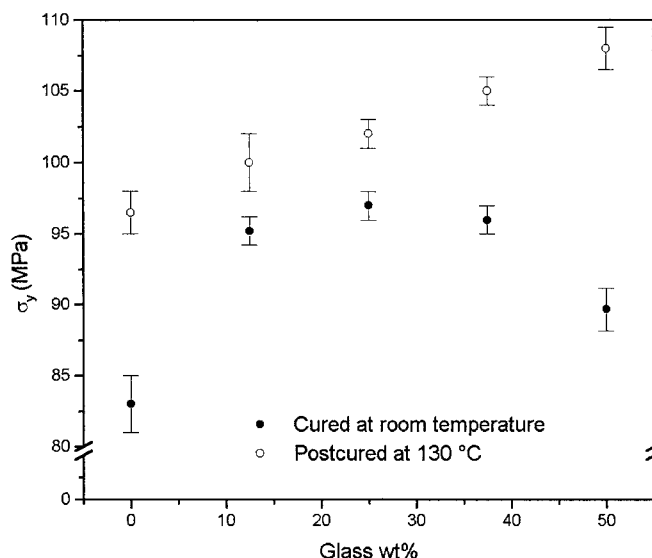


Figure 2. Compressive yield stress vs. wt% glass.

curing treatment as a consequence of the presence of unreacted monomer, which acts as a matrix plasticizer. The results of E for samples having the same proportion of filler cured at room temperature and postcured were statistically analyzed by the t -test (two populations). The analysis revealed that, at the 0.1 level, the two means were significantly different.

Surgical PMMA cement is brittle in nature. Like other brittle materials, it is weak in tension but quite strong in compression²⁹ and capable of yielding under uniaxial compression. Therefore, the yield strength was determined in compression. The values of compressive yield stress (σ_y) for different proportions of filler are shown in Figure 2. The results of σ_y for samples having the same proportion of filler, both cured at room temperature and postcured, were statistically analyzed by the t -test (two populations). The analysis revealed that at the 0.1 level, the two means were significantly different. However, the analysis of the samples having 12.5 and 25 wt% filler and cured at room temperature revealed that, at the 0.05 level, the means were not significantly different. Similarly, the values of the σ_y of samples having 12.5, 25, and 37.5 wt% filler and postcured were not significantly different at the 0.05 level.

By comparing the values obtained in samples cured at room temperature and samples postcured at 130°C, it emerges that free monomer, which decreases with postcure treatment, acts as a matrix plasticizer leading to lower stress values in the case of cements cured at room temperature. For the cements postcured at 130°C, σ_y increased monotonically with filler content. On the contrary, for the cements cured at room temperature having filler content higher than 25 wt%, a drop in σ_y was observed. The fracture toughness of the cements was evaluated according to the ASTM E399 standard by measuring the critical intensity factor (K_{IC}). Plain strain conditions were verified in all test specimens. The results obtained are represented in Figure 3. The results of K_{IC} for samples having the same proportion of filler, both

cured at room temperature and postcured, were statistically analyzed by the t -test (two populations). The analysis revealed that, at the 0.1 level, the two means were significantly different.

K_{IC} increased monotonically with filler content. The cements cured at room temperature reached a K_{IC} value 98% higher than that of the standard cement when 50 wt% filler was added. The materials postcured at 130°C, which are free of unreacted monomer, displayed lower K_{IC} values.

The addition of filler to the polymeric cement produced a monotonic increase in the flexural modulus and the fracture toughness. However, the decrease in the compressive yield strength in materials cured at room temperature having filler content higher than 25 wt% remains to be explained.

PMMA bone cement is a composite polymeric material composed by PMMA spheres embedded within a matrix of recently polymerized MMA monomer. Due to the vitrification phenomenon, the polymerization reaction ceases before consuming the available MMA monomer, that is, the material contains a certain amount of unreacted monomer.³⁰ On the other hand, during the mixing of the components, air bubbles are entrapped into the dough, making the cement porous. Thus, the mechanical behavior of particulate filled bone cements is influenced in a complex way by the porosity, the residual monomer, and the presence of the filler.

As shown in Table I, the replacement of the powder phase of the cement by the filler produced an increase in the L/P ratio. The following measurements were performed to explore changes produced in the polymeric matrix as a consequence of the variation in the L/P ratios. To explain the drop in σ_y (Fig. 2), the polymeric matrix of the composite cements was analyzed by differential scanning calorimetry (DSC) to measure the monomer content in the cured materials. Assuming that the heat produced by MMA polymerization is proportional to the number of monomer units reacted (56.9 kJ/mol),³¹ the monomer content can be measured directly by

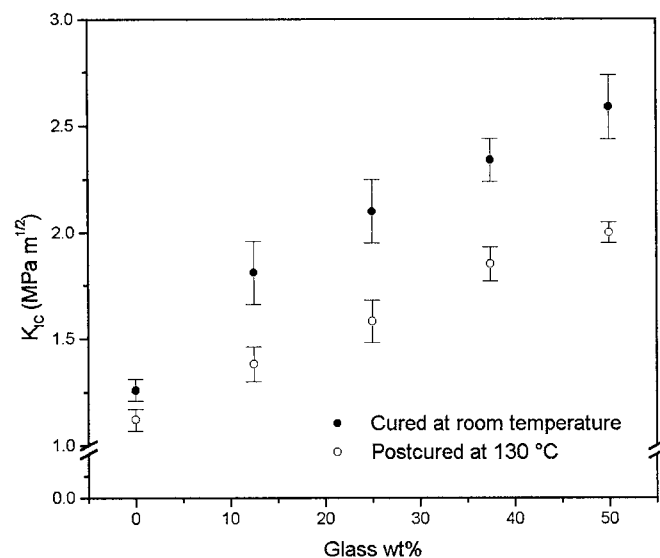


Figure 3. K_{IC} vs. wt% glass.

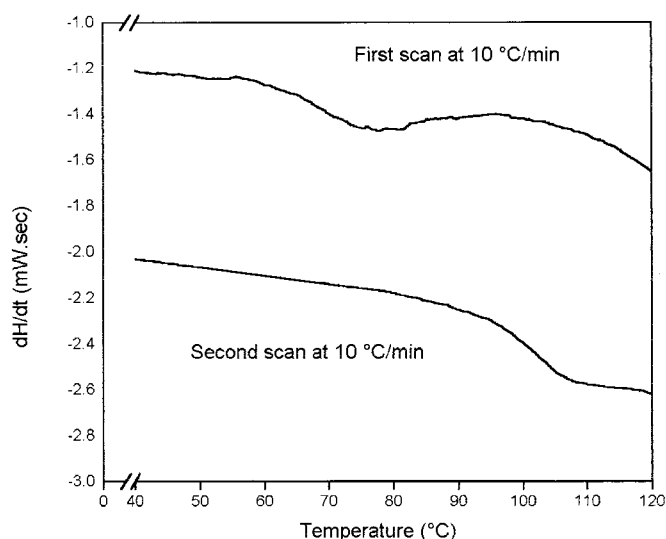


Figure 4. DSC of a sample having L/P = 0.1 cured at room temperature.

DSC. Plaques of bone cement having L/P ratios equal to 0.5, 0.8, and 1 were cured at room temperature. Samples taken from the plaques were scanned from 20–150°C at a heating rate of 10°C/min. Typical DSC thermograms of a sample having L/P = 1 are presented in Figure 4. The traces were shifted over the dH/dt axis in order to show both runs in the same plot. The inflection at approximately 65°C in the first scan corresponds to the glass transition temperature (T_g) of the partially polymerized MMA matrix and the exothermic peak that appears after the T_g corresponds to the reaction heat released by the polymerization of the monomer present in the sample. A second scan of the sample shows the absence of a residual exothermic peak, indicating that the polymerization was completed during the first scan and the inflection corresponds to the T_g of the cured sample. This T_g is the same as the T_g measured for the PMMA powder, which is 105°C.

For the samples having L/P equal to 0.5 and 0.8, the T_g of the partially polymerized MMA matrix and the exothermic peak were not clearly revealed, which can be attributed to a high proportion of PMMA powder with respect to MMA monomer in the initial mix. Therefore, due to the difficulty associated with the sensitivity of the DSC technique, the samples were analyzed by dynamic mechanical analysis (DMA).

The monomer acts as a plastizicer of the matrix, which produces a decrease in the T_g . Figure 5 shows the T_g of bone cement having different monomer content (details of the construction of the vitrification curve were reported elsewhere³⁰). A linear relationship is observed over the range studied. The higher the monomer content, the lower the T_g ; hence, differences in the monomer content of cements having different L/P ratios may be qualitatively estimated by comparing their T_g .

The DMA method defines a precise temperature when DSC transitions become unresolvable from the baseline, and it is approximately 1000 times more sensitive in resolving the

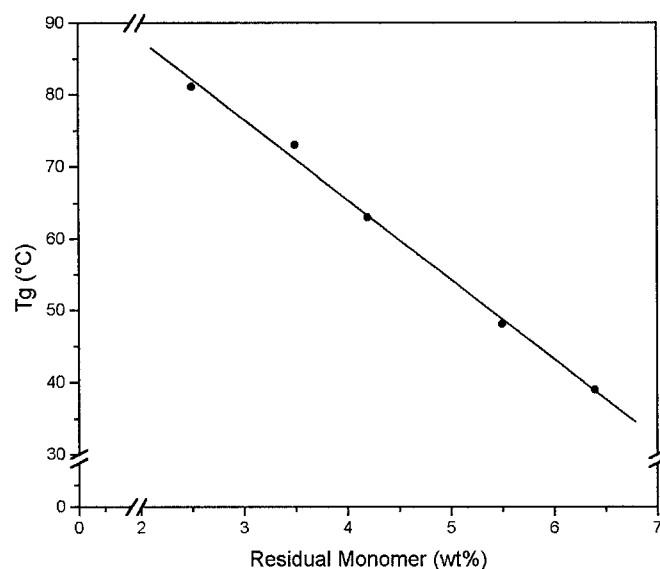


Figure 5. Glass transition temperature vs. the monomer content.

strength of a transition than DSC.³² Moreover, DMA measures molecular motions and not heat changes as DSC. A sharp drop in modulus and probe position accompanied by a peak in $\tan \delta$ during DMA runs indicates the glass-to-rubber transition. Figure 6 is a typical DMA run of a sample having L/P = 0.5. The register of $\tan \delta$ during the test clearly reveals two peaks. The first peak is attributed to the T_g of the partially polymerized MMA matrix and the second peak corresponds to the T_g of the prepolymerized PMMA beads. Differences between the T_g of the PMMA beads measured by DMA and DSC lies in the fact that the $\tan \delta$ peak normally appears at a higher temperature than with the relatively static method of DSC.³² Figure 7 shows DMA traces of samples having L/P ratios equal to 0.5, 0.8, and 1, both cured at room temperature and postured at 130°C. Only the T_g of the partially polymer-

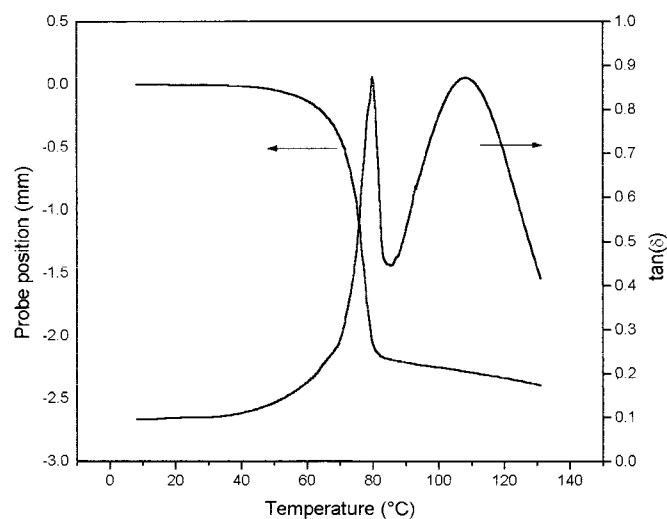


Figure 6. $\tan \delta$ and probe position vs. temperature in a typical DMA run.

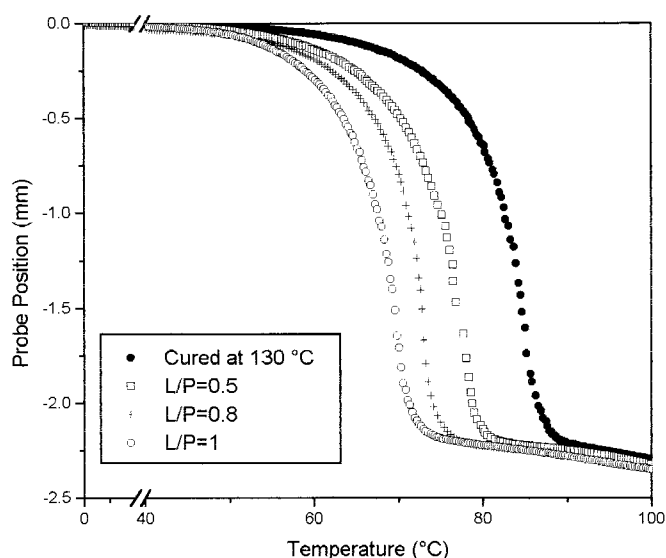


Figure 7. Probe position vs. temperature for samples having different L/P ratios.

ized matrix is shown to make the plot more clear. A decrease of the T_g of the partially polymerized MMA matrix by increasing the L/P ratio can be seen. Figure 8 shows the results of T_g , measured at the $\tan \delta$ peak, vs. L/P. The decrease in T_g with the increase in L/P is attributed to the corresponding increase in the residual monomer content. On the other hand, samples having different L/P ratios and postcured displayed the same T_g values, which is an evidence that the T_g decrease in samples cured at room temperature can be attributed solely to the presence of the monomer.

The effect of the proportion of the components upon compressive and fracture behavior was studied, performing measurements in samples with L/P equal to 0.5 and 0.6. The results are shown in Table II. From the analysis of these

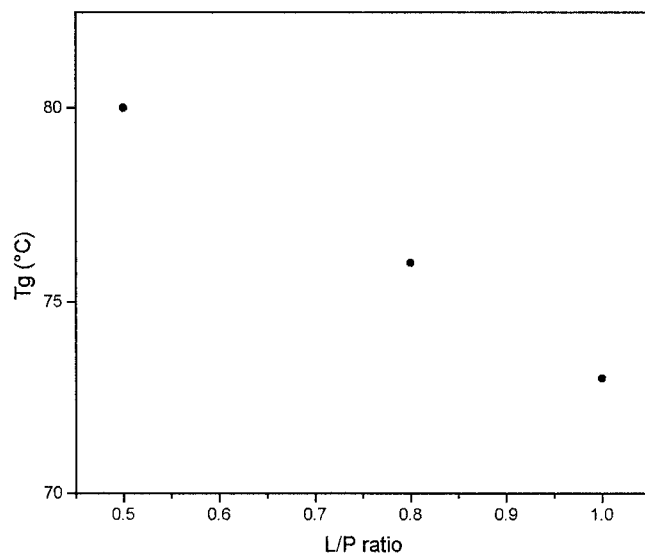


Figure 8. T_g measured at the $\tan \delta$ peak vs. L/P ratio in samples cured at room temperature.

TABLE II. K_{IC} and σ_y of Unreinforced Cements with L/P = 0.5 and 0.6 Cured at Room Temperature and Postcured at 130 °C

| L/P | Cure Cycle | σ_y (Mpa) | K_{IC} (MPa m ^{1/2}) |
|-----|---------------------|------------------|----------------------------------|
| 0.5 | Room Temperature | 82.5 | 1.27 |
| 0.6 | Room Temperature | 69.7 | 1.45 |
| 0.5 | Postcured at 130 °C | 96.5 | 1.12 |
| 0.6 | Postcured at 130 °C | 92.8 | 1.20 |

results, it emerges that, in samples cured at room temperature, when L/P increases σ_y decreases and K_{IC} increases. When yielding occurs at a lower stress, an increase in the size of the plastic zone at the crack tip is expected. The blunting at the crack tip with reduced yield strength tends to improve material toughness. The results of these experiments, however, suggest that unfortunately an increase in toughness resulting from this process is accompanied by a reduction in strength. The materials postcured at 130°C, which are free of unreacted monomer, display lower K_{IC} values, consistent with the increase in σ_y .

In composite cements, the compressive yield strength depends on the strength of both the filler and the matrix. From DMA results, it emerges that, with an increase in filler content, the compressive strength of the matrix decreases as a consequence of an increase in the monomer content. The decrease in the yield strength in samples having filler content higher than 25 wt% may be explained by taking into account that the plasticizing effect of the monomer is not compensated for by the reinforcing effect of the filler. Flexural testing is not as sensitive as compressive or fracture toughness testing in detecting the presence of residual monomer. This fact was reported by previous workers³³ and was evidenced in the present experimental results.

Kim et al.¹⁶ and Vallo et al.²² reported a decrease in the tensile and compressive strength with increased amounts of inorganic particles. As in both works the porosity and pore size increased by increasing the amount of filler, the decrease in strength was explained in terms of porosity. As described later, the porosity of glass-particulate composite cements decreased with the increase in filler proportion. So, the influence of porosity on the decrease in σ_y (Fig. 2) is disregarded.

The analysis of the results reported by previous workers shows that some authors incorporated the filler maintaining the standard L/P ratio equal to 0.5,¹⁵⁻¹⁸ while others incorporated the filler increasing L/P.¹⁹⁻²² From DMA results obtained in the present work, it emerges that the increase in residual monomer produced by increasing L/P must be considered when comparing the overall mechanical behavior of particulate-filled bone cements.

At this point, it is relevant to discuss some aspects related to the experimental procedure of incorporation of particulate fillers to bone cements and its consequences on flow properties and porosity. As the filler acts as a reinforcing agent, it is desirable to incorporate a high proportion of filler to improve the overall mechanical performance of the composite material. The maximum amount of filler that can be added to a

bone cement is limited by the flow properties of the dough, which depends on the viscosity of the initial mix. Cements of low viscosity permit the addition of a higher proportion of filler compared with cements of standard viscosity. Perek et al.²⁰ used a low-viscosity cement and found that 40 wt% of hydroxyapatite filler could be added with an increase in the flow properties relative to the unmodified cement. Khorasani et al.³⁴ and Deb et al.³⁵ reported experimental results of incorporation of 40 wt% of hydroxyapatite to a ductile bone cement with a different formulation and lower viscosity than standard PMMA-based bone cements. On the contrary, the cement used in the present work has a standard viscosity and, as reported previously,²² 15 wt% of hydroxyapatite filler was the maximum proportion that could be incorporated. Materials with higher proportion of filler displayed such low flow properties that the dough could not be molded to make specimens for the mechanical characterization. In clinical practice, the cement must flow into the cancellous bone as pressure is applied. If the viscosity of the dough is too high, the intrusion into the bone interstitial trabeculae is poor, which prevents good mechanical coupling between bone and cement. The success of the implant fixation is associated with the mechanical interlock between the cancellous bone and the cement, which depends on the viscosity of the initial dough. Thus, in some particulate reinforced cements, there is an optimum amount of filler that can be incorporated resulting from a competition between strength and flow properties.

The practice of chilling the constituents of cement formulations prior to mixing is now followed in the clinical setting. This technique prolongs the low viscosity working time of the cement, facilitates its mixing, and maintains the cement in an injectable viscous state after the mixing. In short, it improves the handling of the cement.

Glass-filled bone cements displayed a better workability compared with the traditional cement. The explanation is that the increase in L/P produces a better wettability of the powder phase, which results in a decrease of the viscosity of the initial mix. Moreover, with an increase in the L/P ratio, the amount of PBO initiator present in the powder phase decreases, and the amount of hydroquinone inhibitor present in the liquid phase increases, which results in a longer dough time. The decrease in the viscosity facilitates the escaping of air bubbles embodied during the mixing, and the longer dough time gives enough time to accomplish the removal of the air bubbles by methods such as vacuum mix or centrifugation of the dough after mixing. Both factors contribute to a decrease in the porosity of the cured material. Despite that the porosity was not quantitatively determined, the use of a radiolucent cement allowed a qualitative evaluation. Visual inspection revealed that, by increasing the filler proportion, that is, increasing L/P, the porosity was markedly reduced and the presence of macropores was not observed.

On the other hand, the filler characteristics also influence the porosity of the hardened material. Kim et al.¹⁶ studied the effect of the incorporation of bone mineral particles on bone cement porosity. The authors reported that the pore size increased by increasing the amount of filler. Similar results

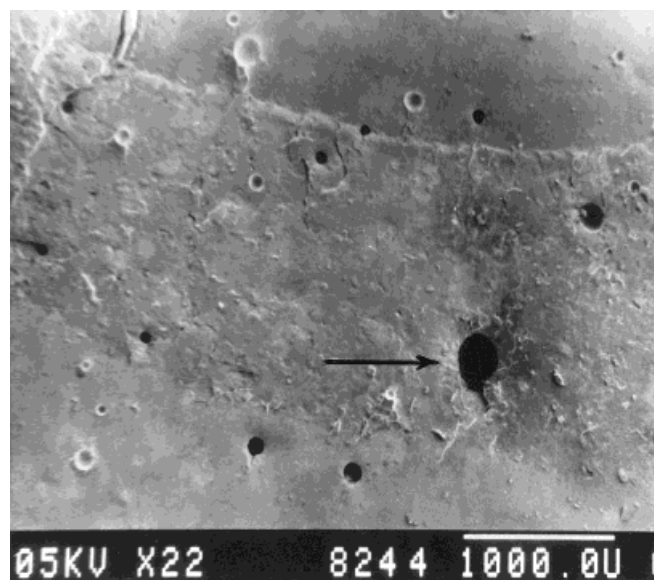


Figure 9. SEM micrograph of the fracture surface of the unreinforced cement. A void present in the material is indicated by the black arrow.

were reported by Vallo et al.²² on the incorporation of hydroxyapatite particles to bone cement. Bone mineral particles and hydroxyapatite particles are quite porous by themselves and absorb monomer initially when the components are mixed. Because there is not enough liquid to properly wet the powder, the viscosity of the paste increases giving as a result a highly porous material. Glass particles are not porous, so the viscosity of the paste is not affected by this type of filler. From these observations, it emerges that the decrease observed in the porosity of glass-reinforced cements is a consequence of a decrease in the viscosity of the initial mix and the surface characteristic of the glass particles.

The surfaces of the cements cured at room temperature and used in the fracture toughness measurements were analyzed to elucidate the deformation mechanisms that contributed to the increase in K_{IC} .

Visual examination of the fracture surfaces of the conventional bone cement revealed that the crack showed flat propagation with a brittle aspect. Figure 9 is the SEM micrograph of a general view in a region near the notch for the standard cement. The presence of zones of different features can be observed with an abrupt transition between them. The zones are associated with different propagation crack modes. The very smooth “mirror-like” zone is associated with rapid crack propagation regions, and the rougher zone with slow crack propagation and arrest. It is well known that crazing is the main mechanism responsible for plastic deformation in PMMA when stressed in tension. Standard bone cement samples exhibited stress whitening, which arises from the development of crazes before crack propagation.

The addition of a filler produced a significant change in the fracture surface aspect compared with the unreinforced cement. Fracture surfaces of reinforced cements were macroscopically very rough and three-dimensional, which is indicative of crack branching. The increase of plastic deformation

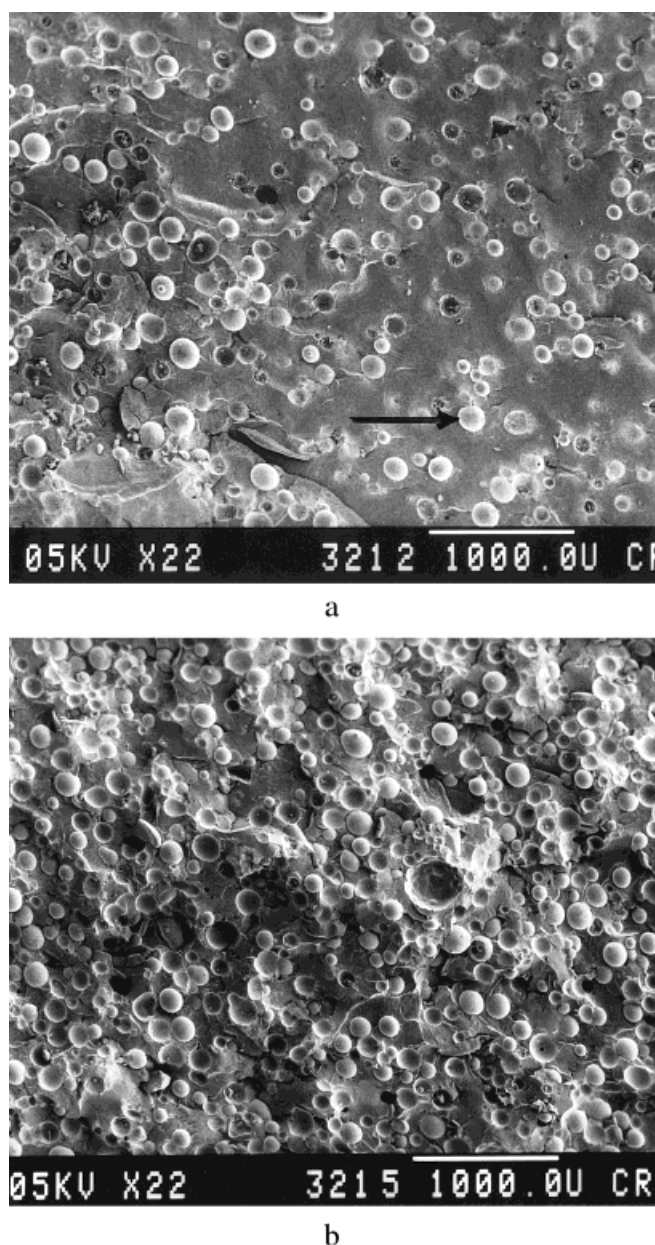


Figure 10. (a)–(b) SEM micrographs of the fracture surface of the cement containing 37.5 and 50 wt% glass particles, respectively. The filler particles, indicated by the black arrow, appear almost perfectly spherical, and there is a good distribution of particles and no aggregation or settlement in the material.

of the cement matrix with filler content could even be detected macroscopically, because the plastically deformed zone ahead of the crack tip exhibited stress whitening. The size of the stress-whitened zone increased with the filler content, which indicated that extensive crazing had occurred. The particles of the powder phase of the cement are not clearly seen in the SEM micrographs shown in Figures 9–12, because their diameters range between 5–50 μm . As shown in a previous work,³⁰ they are seen at higher magnification.

Figures 10 (a)–(b) show SEM micrographs of cements containing 37.5 wt% and 50 wt% filler, respectively. The

filler particles appear almost perfectly spherical, and it can be seen that there is a good distribution of particles and no aggregation or settlement in the material. Bonding between glass spheres and acrylic bone cement is poor, indicated by the smooth appearance of the glass surfaces shown protruding above the fracture plane of the acrylic matrix. No matrix could be seen attached to the surface of pulled-out glass spheres, and a large number of glass hemispheres beneath the fracture surface of the matrix had clearly separated from the acrylic material. The interfacial debonding between glass and matrix is more clearly seen in Figure 11, which was taken at a higher magnification. The rough fracture surface is due to the crack propagation in layers of crazed material below and above the main crack plane. Ridges are formed by the merging of two crack planes at slightly different levels. This occurs when the crack front passes around a particle, splitting the crack, which then travels on two different planes. The bifurcated crack merges again after passing the particle forming a ridge. Figures 12 (a)–(b) show detailed views of the cement containing 50 wt% filler. Plastically deformed material is evident at this higher magnification. The rough structure with prominences and depressions caused by variations in the crack propagation can be seen above and below the main crack plane.

The incorporation of rigid particulate fillers into the bone cement provokes a notable increase in toughness, as seen in Figure 3. There are several mechanisms that might be responsible for toughening in particle-reinforced polymers.

In the first place, one way to increase the toughness of a composite material is to promote the mechanisms of energy absorption of the polymeric matrix, like crazing and micro-cracking in the damage zone ahead of the crack tip. In this way, the amount of energy absorption prior to fracture is increased, making it less probable that a crack attains the

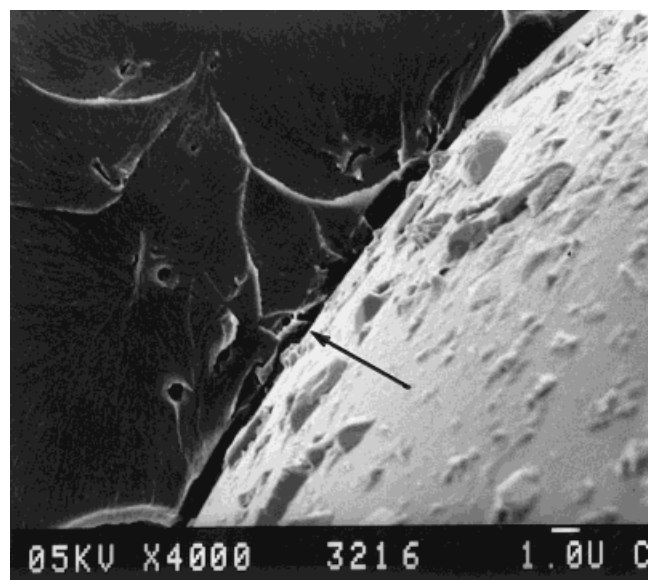


Figure 11. SEM micrograph taken at high magnification showing a poor degree of adhesion between the polymeric matrix and the glass filler. The matrix–particle interface is indicated by the black arrow.

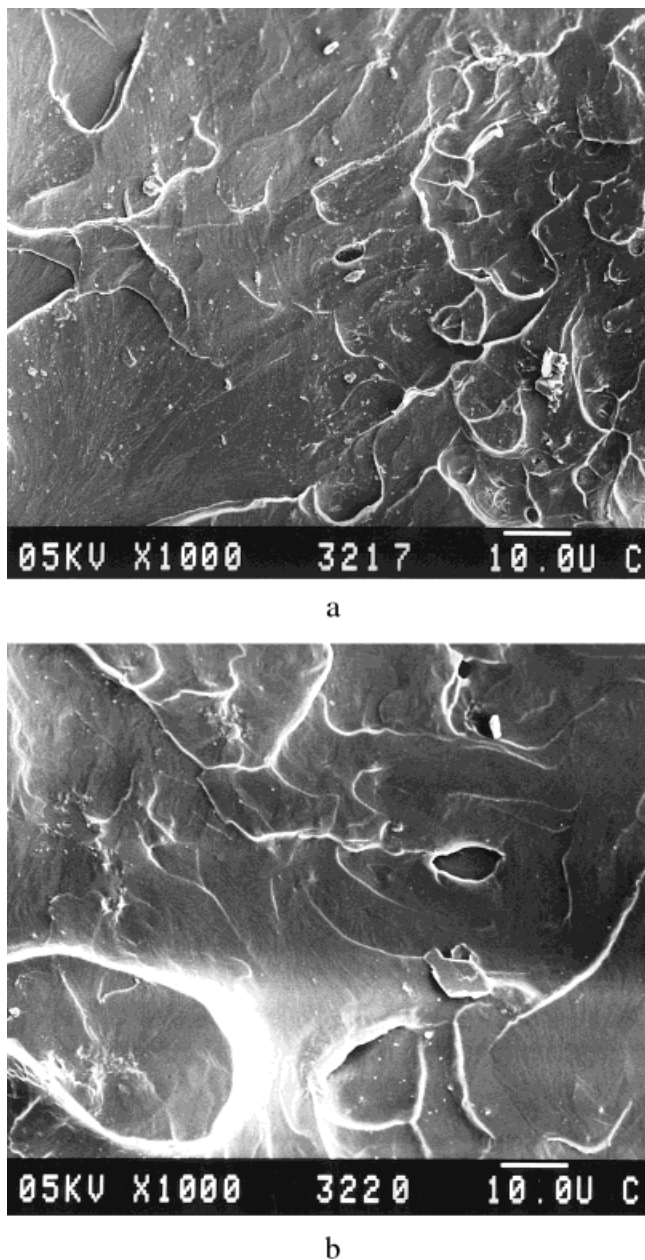


Figure 12. (a)–(b) SEM micrograph of the fracture surface of the cement containing 50 wt% glass particles taken at a higher magnification than in Fig. 10. Plastically deformed material is evident at this higher magnification. A rough structure is visible, with prominences and depressions caused by variations in the crack propagation above and below the main crack plane.

critical length for fracture. The work required to stretch crazes at the crack tip is a lineal function of the number of crazes nucleated.²⁸ Under tensile stresses, the crazes tend to be nucleated in the sites with maximum tri-axial stress concentration, which are generally near the maximum diameter of the glass particles. From these places, they tend to grow perpendicularly to the maximum principal stress and deviate when they interact with stress fields of other particles. The filler particles are nucleation sites for crazes or microcracks, which extend the damage zone. Hence, an increase in filler

content should result in increased crazing and fracture toughness, as observed.

On the other hand, by the action of the rigid particulate filler, the toughness of the acrylic matrix is enhanced by promoting interactions between the moving crack front and the second phase dispersion. When a crack begins to propagate within a material, the rigid particles act as obstacles and the crack front bows outwards between two particles before breaking free. The crack front elongates as it bows out, absorbing fracture energy. This mechanism has been previously described in the literature as crack pinning.²⁸ The presence of tails behind the particles is often taken as an indication that pinning of the crack front has taken place (Fig. 10). However, the absence of tails does not necessarily mean that no pinning occurred, because at high weight fractions of particles there may be considerable overlap of the secondary cracks.³⁶ Beaumont¹⁵ studied the strength and toughness of acrylic bone cements containing a second phase dispersion of glass spheres. Measurements of K_{IC} as a function of glass content (V_p) demonstrated that K_{IC} increased with V_p and reached a peak at $V_p = 0.25$. The author attributed the increase in K_{IC} up to $V_p = 0.25$ to a crack front-glass sphere interaction effect and concluded that the glass spheres acted as obstacles to crack extension.

Another fundamental mechanism of toughening is crack tip blunting. Material at the crack tip, which deforms plastically, reduces the stress intensity and, hence, decreases the driving force for crack extension. The decrease in σ_y of the polymeric matrix with increasing filler content promotes the blunting at the crack tip, which produces an increase in K_{IC} . In addition, decohesion of the particles from the matrix in front of the crack tip also gives rise to crack tip blunting.³⁶ As the crack propagates the particles debond, which provokes crack tip blunting giving, as a result, higher values of toughness compared to well-bonded particles. Thus, debonding of the particles from the cement is an available energy release mechanism to delay crack propagation.

The activation of the aforementioned mechanisms of deformation by the incorporation of filler leads to an increase of the absorbed energy and explains the rise in fracture toughness.

It must be considered that porosity can promote different mechanisms on the crack propagation behavior.^{37–40} However, Topoleski et al. demonstrated that these mechanisms could be significant only under fatigue loading conditions, because under static loading conditions the stress concentration from porosity is negligible compared to the stress intensity at the crack tip.³⁹

It may be concluded that the addition of glass particles to a bone cement resulted in a significant improvement in its mechanical properties. However the cyclic nature of joint loading implies fatigue as a critical step leading to eventual failure. Thus, further research will study the fatigue behavior of glass-filled bone cements. Furthermore, it is necessary to optimize the amount of filler to maintain good mechanical performance and favorable tissue response. Therefore, *in vivo* experiments are certainly necessary to determine if the higher

residual monomer compared with the traditional cement could jeopardize tissue tolerance. The markedly improved mechanical performance measured under static loading conditions encourages further research.

CONCLUSIONS

A commercial acrylic bone cement was modified by the incorporation of different weight fractions of glass spheres. It was found that up to 50 wt% glass particles could be added without compromising the flow properties of the composite cements. The addition of filler to the bone cement resulted in a significant improvement in its mechanical properties. DMA analysis revealed an increase in residual monomer content with increasing filler proportion. The unreacted monomer acts as a plasticizer, which reduces the compressive strength and increases K_{IC} . The observed increase in fracture toughness could be rationalized through the application of proposed mechanisms for toughening of particle-reinforced polymers.

The financial support provided by the National Research Council (CONICET) is gratefully acknowledged. Appreciation is extended to Mr. Juan Asarou for his assistance in preparing samples for mechanical characterization.

REFERENCES

- Lewis G. Properties of acrylic bone cement: state of the art review. *J Biomed Mater Res Appl Biomater* 1997;38:155–182.
- Eyrer P, Jin R. Influence of mixing technique on some properties of PMMA bone cements. *J Biomed Mater Res* 1986;20:1057–1094.
- Kindt-Larsen T, Smith D, Jensen JS. Innovation in acrylic bone cement and application equipment. *J Biomed Mater Res Appl Biomater* 1995;6:75–83.
- Müller-Wille P, Wang JS, Lidgren L. Integrated system for preparation of bone cement and effects on cement quality and environment. *J Biomed Mater Res Appl Biomater* 1997;38:135–142.
- Lewis G, Nyman JS, Triew HH. Effect of mixing method on selected properties of acrylic bone cement. *J Biomed Mater Res Appl Biomater* 1997;38:221–228.
- Lidgren L, Drar H, Möller J. Strength of polymethylmethacrylate increased by vacuum mixing. *Acta Orthop Scand* 1984;55:536–541.
- Rimnac C, Wright T, McGill D. The effect of centrifugation on the fracture properties of acrylic bone cements. *J Bone Joint Surg* 1986;68A:281–287.
- Lewis G, Austin G. Mechanical properties of vacuum-mixed acrylic bone cement. *J Biomed Mater Res Appl Biomater* 1994;5:307–314.
- Wang JS, Toksvig-Larsen S, Müller-Wille P, Franzén H. Is there any difference between vacuum mixing systems in reducing bone cement porosity? *J Biomed Mater Res Appl Biomater* 1996;33:115–119.
- Beaumont PWR, Young RJ. Slow crack growth in acrylic bone cements. *J Biomed Mater Res* 1975;9:423–439.
- Saha S, Pal S. Improvement of mechanical properties of acrylic bone cement by fiber reinforcement. *J Biomechan* 1984;17:467–478.
- Pourdeyhimi B, Wagner HD. Elastic and ultimate properties of acrylic bone cement reinforced with ultra high molecular-weight polyethylene fibers. *J Biomed Mater Res* 1989;23:63–80.
- Topoleski LDT, Ducheyne P, Cuckler JM. The fracture toughness of titanium-fiber-reinforced bone cement. *J Biomed Mater Res* 1992;26:1599–1617.
- Gilbert JL, Net SS, Lautenschlager EP. Self-reinforced composite poly(methylmethacrylate): static and fatigue properties. *Biomater* 1995;16:1043–1055.
- Beaumont PWR. The strength of acrylic bone cement and acrylic cement-stainless steel interfaces. *J Mater Sci* 1977;12:1845–1852.
- Kim YS, Kang YH, Kim JK, Park JB. The effect of bone mineral particles on the porosity of bone cement. *Biomed Mater Eng* 1994;4:37–46.
- Harper EJ, Behiri JC, Bonfield W. Flexural and fatigue properties of a bone cement based upon polyethylmethacrylate and hydroxyapatite. *J Mater Sci Mater Med* 1995;6:799–903.
- Vila MM, Ginebra MP, Gil FJ, Planell JA. Effect of porosity and environment on the mechanical behavior of acrylic bone cement modified with acrylonitrile-butadiene-styrene particles: Part I. Fracture toughness. *J Biomed Mater Res Appl Biomater* 1999;48:121–127.
- Castaldini A, Cavallini A, Cavalcoti D. Microstructure and mechanical properties of polymethylmethacrylate composite cements. Pizzoferrato A, Marchetti PG, Ravaglioli A, Lee AJC, editors. *Biomaterials and clinical applications*. Amsterdam: Elsevier Science; 1987. p 517–522.
- Perek J, Pilliar RM. Fracture toughness of composite acrylic bone cements. *J Mater Sci Mater Med* 1992;3:333–334.
- Murakami A, Behiri JC, Bonfield W. Rubber-modified bone cements. *J Mater Sci* 1988;23:2029–2036.
- Vallo CI, Montemartini PM, Fanovich MA, Porto López JM, Cuadrado TR. Polymethylmethacrylate-based bone cement modified with hydroxyapatite. *J Biomed Mater Res Appl Biomater* 1999;48:150–158.
- Vila MM, Ginebra MP, Gil FJ, Planell JA. Effect of porosity and environment on the mechanical behavior of acrylic bone cement modified with acrylonitrile-butadiene-styrene particles: Part II. Fracture toughness. *J Biomed Mater Res Appl Biomater* 1999;48:128–134.
- Castaldini A, Cavallini A. Creep behavior of composite bone cements. Christel P, Munier A, Lee AJC, editors. *Biological and biomedical performance of biomaterials*. Amsterdam: Elsevier Science; 1986. p 525–530.
- Clark AE, Anusavice KJ. Dental applications of glasses. *Eng Mater Hndbk* 1989;4:1091.
- Beaumont PWR. Fracture processes in acrylic bone cement containing barium sulphate dispersions. *J Biomed Eng* 1979;1:147–152.
- Owen AB, Beaumont PWR. Fracture behaviour of commercial surgical acrylic bone cements. *J Biomed Eng* 1978;1:277–280.
- Kinloch AJ, Young RJ. Fracture behavior of polymers. Essex, England: Applied Science; 1983.
- Vallo CI, Cuadrado TR, Frontini PM. Mechanical and fracture behaviour evaluation of commercial acrylic bone cements. *Polym Int* 1997;43:260–268.
- Vallo CI, Montemartini PE, Cuadrado TR. Effect of residual monomer content on some properties of a poly(methylmethacrylate)-based bone cement. *J Appl Polym Sci* 1998;69:1367–1383.
- Turi A, editor. *Thermal characterization of polymeric materials*. London: Academic; 1981.
- Hunt BJ, James MI, editors. *Polymer characterization*. London: Chapman Hall; 1997.
- Moloney AC, Kausch HH, Stieger HR. The fracture of particulate-filled epoxide resins. *J Mater Sci* 1984;19:1125–1230.

34. Khorasni SN, Deb S, Behiri JC, Braden M, Bonfield W. Modified hydroxyapatite reinforced PEMA bone cement. *Bioceram* 1992;5:225–232.
35. Deb S, Braden M, Bonfield W. Water absorption characteristics of modified hydroxyapatite bone cements. *Biomater* 1995;16:1095–1100.
36. Spanoudakis J, Young RJ. Crack propagation in a glass particle-filled epoxy resin. *J Mater Sci* 1984;19:473–486.
37. Lewis G. Effect of mixing and storage temperature of cement constituents on the fatigue and porosity of acrylic bone cement. *J Biomed Mater Res Appl Biomater* 1999;48:143–149.
38. Topoleski LDT, Ducheyne P, Cuckler JM. A fractographic analysis of in vivo poly(methylmethacrylate) bone cement failure mechanisms. *J Biomed Mater Res Appl Biomater* 1990;24:135–154.
39. Topoleski LDT, Ducheyne P, Cuckler JM. Microstructural pathway of fracture in poly(methylmethacrylate) bone cement. *Biomater* 1993;14:1165–1172.
40. Lewis G. Relative roles of cement molecular weight and mixing methods on the fatigue performance of acrylic bone cement: Simplex® P versus Osteopal®. *J Biomed Mater Res Appl Biomater* 2000;53:119–130.